AD-A179 179 A CONSISTENT FINITE ELEMENT FORMULATION OF NONLINEAR 1/1
FRICTIONAL CONTACT P (U) CALIFORNIA UNIV BERKELEY DEPT
OF CIVIL ENGINEERING J JU ET AL MAR 87 NCEL-CR-87.008
UNCLASSIFIED N62583-86-M-T167 F/G 20/11 NL

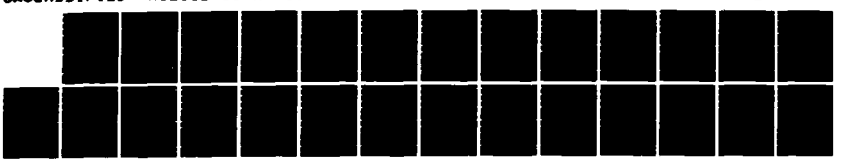

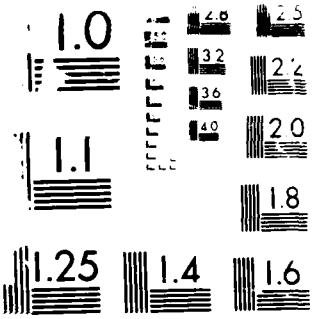
1.0
1.1
1.25
1.4
1.6
1.8
2.0
2.2
2.5
2.8
3.2
3.6
4.0

CR 87.008
March 1987

NCEL
Contract Report

An Investigation Conducted By University of California, Berkeley, Department of Civil Engineering

Sponsored By Naval Facilities Engineering Command

A CONSISTENT FINITE ELEMENT FORMULATION OF NONLINEAR FRICTIONAL CONTACT PROBLEMS

ABSTRACT A perturbed Lagrangian-based variational formulation is proposed for the finite element solution of fully nonlinear frictional contact problems. In the spirit of an operator splitting methodology, an analogy exists between the proposed treatment for the stick-slip motion and the corresponding treatment in elastoplasticity.

Within the context of discrete formulations arising from a finite element approximation, explicit expressions for the frictional consistent contact tangent stiffness and residual are derived from variational equations by using a consistent linearization procedure for both the sliding and adhesion phases. The consistent tangent operator is always non-symmetric for the case of frictional sliding owing to the nature of the Coulomb's friction law employed.

For two-dimensional applications, a three-node contact element is employed in the finite element discretization. Numerical examples are also presented that illustrate the performance of the proposed formulation.

Keywords: Structural mechanics

NAVAL CIVIL ENGINEERING LABORATORY PORT HUENEME CALIFORNIA 93043

METRIC CONVERSION FACTORS

Approximate Conversions to Metric Measures

Symbol	When You Know	Multiply by	To Find	Symbol
		LENGTH		
in	inches	*2 5	centimeters	cm
ft	feet	30	centimeters	cm
yd	yards	0.9	meters	m
mi	miles	1.6	kilometers	km
		AREA		
in^2	square inches	6 5	square centimeters	cm^2
ft^2	square feet	0 09	square meters	m^2
yd^2	square yards	0 8	square meters	m^2
mi^2	square miles	2 6	square kilometers	km^2
	acres	0.4	hectares	ha
		MASS (weight)		
oz	ounces	28	grams	g
lb	pounds	0.45	kilograms	kg
	short tons (2,000 lb)	0.9	tonnes	t
		VOLUME		
tsp	teaspoons	5	milliliters	ml
Tbsp	tablespoons	15	milliliters	ml
fl oz	fluid ounces	30	milliliters	ml
c	cups	0.24	liters	l
pt	pints	0.47	liters	l
qt	quarts	0.95	liters	l
gal	gallons	3.8	liters	l
ft^3	cubic feet	0.03	cubic meters	m^3
yd^3	cubic yards	0.76	cubic meters	m^3
		TEMPERATURE (exact)		
°F	Fahrenheit temperature	5/9 (after subtracting 32)	Celsius temperature	°C

*1 in = 2.54 (exactly). For other exact conversions and more detailed tables, see NBS Misc. Publ. 286, Units of Weights and Measures, Price $2.25, SD Catalog No. C13.10:286.

Approximate Conversions from Metric Measures

Symbol	When You Know	Multiply by	To Find	Symbol
		LENGTH		
mm	millimeters	0 04	inches	in
cm	centimeters	0.4	inches	in
m	meters	3.3	feet	ft
m	meters	1.1	yards	yd
km	kilometers	0.6	miles	mi
		AREA		
cm^2	square centimeters	0.16	square inches	in^2
m^2	square meters	1.2	square yards	yd^2
km^2	square kilometers	0.4	square miles	mi^2
ha	hectares (10,000 m^2)	2.5	acres	
		MASS (weight)		
g	grams	0.035	ounces	oz
kg	kilograms	2.2	pounds	lb
t	tonnes (1,000 kg)	1.1	short tons	
		VOLUME		
ml	milliliters	0.03	fluid ounces	fl oz
l	liters	2.1	pints	pt
l	liters	1.06	quarts	qt
l	liters	0.26	gallons	gal
m^3	cubic meters	35	cubic feet	ft^3
m^3	cubic meters	1.3	cubic yards	yd^3
		TEMPERATURE (exact)		
°C	Celsius temperature	9/5 (then add 32)	Fahrenheit temperature	°F

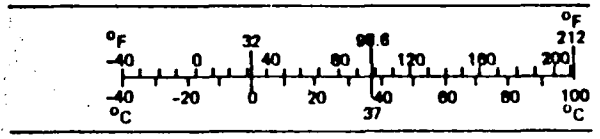

DISCLAIMER NOTICE

THIS DOCUMENT IS BEST QUALITY PRACTICABLE. THE COPY FURNISHED TO DTIC CONTAINED A SIGNIFICANT NUMBER OF PAGES WHICH DO NOT REPRODUCE LEGIBLY.

Unclassified

SECURITY CLASSIFICATION OF THIS PAGE (When Data Entered)

REPORT DOCUMENTATION PAGE	READ INSTRUCTIONS BEFORE COMPLETING FORM
1 REPORT NUMBER: CR 87.008	2 GOVT ACCESSION NO. / 3 RECIPIENT'S CATALOG NUMBER
4 TITLE (and Subtitle): A Consistent Finite Element Formulation of Nonlinear Frictional Contact Problems	5 TYPE OF REPORT & PERIOD COVERED: Final, Mar 1986 - Feb 1987 / 6 PERFORMING ORG. REPORT NUMBER
7 AUTHOR(s): Jiann-wen Ju, Robert L. Taylor, Louis Y. Cheng	8 CONTRACT OR GRANT NUMBER(s): N62583/86-MT167
9 PERFORMING ORGANIZATION NAME AND ADDRESS: Department of Civil Engineering, University of California, Berkeley	10 PROGRAM ELEMENT, PROJECT, TASK AREA & WORK UNIT NUMBERS: 61153N, YR023.03.01.001
11 CONTROLLING OFFICE NAME AND ADDRESS: Naval Civil Engineering Laboratory, Port Hueneme, CA 93043-5003	12 REPORT DATE: March 1987 / 13 NUMBER OF PAGES: 34
14 MONITORING AGENCY NAME & ADDRESS (if different from Controlling Office): Naval Facilities Engineering Command, 200 Stovall Street, Alexandria, VA 22332-2300	15 SECURITY CLASS (of this report): Unclassified / 15a DECLASSIFICATION DOWNGRADING SCHEDULE
16 DISTRIBUTION STATEMENT (of this Report): Approved for public release; distribution is unlimited.	
17 DISTRIBUTION STATEMENT (of the abstract entered in Block 20, if different from Report)	
18 SUPPLEMENTARY NOTES	
19 KEY WORDS (Continue on reverse side if necessary and identify by block number): finite element, contact problems, friction, structural mechanics	

20 ABSTRACT (Continue on reverse side if necessary and identify by block number)

A perturbed Lagrangian-based variational formulation is proposed for the finite element solution of fully nonlinear frictional contact problems. In the spirit of an operator splitting methodology, an analogy exists between the proposed treatment for the stick-slip motion and the corresponding treatment in elastoplasticity.

DD FORM 1473 EDITION OF 1 NOV 65 IS OBSOLETE

Unclassified

SECURITY CLASSIFICATION OF THIS PAGE (When Data Entered)

Within the context of discrete formulations arising from a finite element approximation, explicit expressions for the frictional consistent contact tangent stiffness and residual are derived from variational equations by using a consistent linearization procedure for both the sliding and adhesion phases. The consistent tangent operator is always non-symmetric for the case of frictional sliding owing to the nature of the Coulomb's friction law employed.

For two-dimensional applications, a three-node contact element is employed in the finite element discretization. Numerical examples are also presented that illustrate the performance of the proposed formulation.

TABLE OF CONTENTS

1. Introduction 2

2. Discrete variational formulation 3

2.1 Finite element discretization 3

2.2 Frictional stick. 4

2.3 Frictional slip 7

3. Numerical implementation and examples 8

3.1 Finite element implementation 8

3.2 Example 1: frictional stick 9

3.3 Example 2: frictional slide 10

4. Conclusion 11

Acknowledgments 11

References 12

1. Introduction

Frictional stick-slip contact phenomena constitute important aspects of real engineering applications. The micromechanics of friction for metallic surfaces in contact has drawn significant attention in the literature during the past several decades. Basically, the contact surfaces are not smooth planes but rough, uneven surfaces composed of many *asperities*. Microstructurally, the asperities experience local yielding and fracture. Moreover, they determine the *real* area of contact as opposed to the *nominal* area of contact. For a review on the physical aspects of friction, see for example Tabor [1981], Oden & Martins [1985] and Oden & Pires [1984].

For a finite element solution frictionless contact problems, a perturbed Lagrangian and an augmented Lagrangian formulations have been proposed by Simo, Wriggers & Taylor [1985], and Landers & Taylor [1985], respectively. On the other hand, Duvaut & Lions [1976], Oden & Martins [1985], and Oden & Lin [1986] have proposed some regularization techniques of the Coulomb's law of friction for numerical solution of dynamic frictional contact phenomena.

In this study, a *perturbed Lagrangian*-based formulation is proposed for the finite element solution of fully *nonlinear* frictional contact problems. The stick-slip contact phenomena is accommodated by means of a nonlinear variational formulation. In view of an analogy between the Coulomb's law of friction for the stick-slip motion and the yield criterion for classical elastoplasticity (see, e.g., Michalowski & Mroz [1978]), a two-step operator splitting methodology is employed.

In the current literature, the modification of the tangent stiffness accounting for the contribution of frictional contact often takes the form of symmetric and/or non-symmetric *rank-one* updates inherited from the *linear* theory (see, e.g., Oden & Martins [1985] and Hughes *et al.* [1976]). In the finite element solution of geometrically nonlinear frictional contact problems, however, such simple procedures are no longer adequate. In the event of frictionless contact, a consistent tangent operator has been obtained by Wriggers & Simo [1985].

Within the context of finite element discrete approximation, explicit expressions for the frictional contact tangent stiffness and the residual are derived in this paper from variational equations by using a *consistent linearization* procedure for both the sliding and adhesion phases. It is shown that for the case of frictional stick the consistent tangent operator is symmetric *only* when numerical convergence is achieved. On the other hand, the consistent tangent operator is *always* non-symmetric for the case of frictional sliding owing to the nature of the Coulomb's friction law employed. Not surprisingly, these expressions degenerate to the classical rank-one corrections of the stiffness matrices in the limiting case of infinitesimal deformations. It is emphasized that, in the presence of nonlinear contact kinematics, use of the consistent contact tangent stiffness is essential in preserving the quadratic rate of asymptotic convergence of Newton's method.

For two-dimensional applications, a three-node contact element is employed in the finite element discretization. The "perturbed Lagrangian"-based computational algorithm is capable

of performing a one-pass or two-pass contact slide-line logic. A number of numerical examples are presented in Sec. 3 that illustrate the performance of the proposed variational formulation.

2. Discrete variational formulation

Within the framework of the finite element method, the governing variational equations involving fully nonlinear kinematics are considered in this section for both adhesive and sliding contact problems. In what follows, for simplicity, attention is focused on the two-dimensional (planar) geometry. The extension to three-dimensional geometry is complicated by geometric considerations only.

2.1. Finite element discretization

Throughout the remaining part of this report, we employ the bilinear isoparametric elements for "parent" contacting bodies. Concerning the contact segment characterization, the "master-slave" slide-line contact logic is adopted (see Hallquist [1983]). In particular, a three-node contact element, consisting of two "master" nodes and one "slave" node, is used, see Figure 1. With reference to Figure 1, the tangent and normal vectors are defined as follows:

$$\mathbf{t} \equiv \frac{\mathbf{x}_2 - \mathbf{x}_1}{|\mathbf{x}_2 - \mathbf{x}_1|} \tag{2.1}$$

$$\mathbf{n} \equiv \mathbf{e}_3 \times \mathbf{t} \ , \tag{2.2}$$

where $\mathbf{e}_3$ denotes the unit base vector normal to the plane of the three-node element and $\mathbf{x}_1 = \mathbf{X}_1 + \mathbf{u}_1$, $\mathbf{x}_2 = \mathbf{X}_2 + \mathbf{u}_2$ signify the *current* positions of the master nodes ($\mathbf{X}_1$, $\mathbf{X}_2$ for reference coordinates and $\mathbf{u}_1$, $\mathbf{u}_2$ for current nodal dispacements). In addition, we define the current "surface coordinate" a as follows

$$a \equiv \frac{(\mathbf{x}_s - \mathbf{x}_1)}{|\mathbf{x}_s - \mathbf{x}_1|} \cdot \mathbf{t} \tag{2.3}$$

in which $\mathbf{x}_s = \mathbf{X}_s + \mathbf{u}_s$ denotes the current position of the slave node. The normal and tangential gaps (penetrations) associated with a typical three-node element are defined as

$$g_n \equiv (\mathbf{x}_s - \mathbf{x}_1) \cdot \mathbf{n} \tag{2.4}$$

$$g_t \equiv (\mathbf{x}_s - \mathbf{x}_1) \cdot \mathbf{t} - a^0 \ |\mathbf{x}_2 - \mathbf{x}_1| \ , \tag{2.5}$$

where a^0 is the (old) surface coordinate at the last time step (known). The variations (increments) of the normal and tangent vectors due to *nonlinear* kinematics can be shown to be (see Wriggers & Simo [1985])

$$\delta\mathbf{n} = \frac{-1}{|\mathbf{x}_2 - \mathbf{x}_1|} (\mathbf{t} \otimes \mathbf{n}) \cdot (\boldsymbol{\eta}_2 - \boldsymbol{\eta}_1) \tag{2.6}$$

$$\delta\mathbf{t} = \frac{1}{|\mathbf{x}_2 - \mathbf{x}_1|} (\mathbf{n} \otimes \mathbf{n}) \cdot (\boldsymbol{\eta}_2 - \boldsymbol{\eta}_1) \tag{2.7}$$

where $\boldsymbol{\eta}$ is the variation (increment) of $\mathbf{u}$. Furthermore, for convenience, we define the following abbreviations (operators)

$$\overline{(\bullet)} \equiv (\bullet)_s - (1-a)(\bullet)_1 - a\,(\bullet)_2 \tag{2.8a}$$

$$\overline{\overline{(\bullet)}} \equiv (\bullet)_2 - (\bullet)_1 \tag{2.8b}$$

With the above notations at hand, we now give the variational derivation.

2.2. Frictional stick

For the case of frictional stick (no-slip), we consider the following *perturbed Lagrangian* functional for bodies in contact:

$$\overline{\Pi}_\omega(\mathbf{u}\ ,\ \boldsymbol{\Lambda}_n\ ,\ \boldsymbol{\Lambda}_t) = \Pi(\mathbf{u}) + \boldsymbol{\Lambda}_n^T\mathbf{G}_n - \frac{1}{2\omega_n}\boldsymbol{\Lambda}_n^T\boldsymbol{\Lambda}_n + \boldsymbol{\Lambda}_t^T\mathbf{G}_t - \frac{1}{2\omega_t}\boldsymbol{\Lambda}_t^T\boldsymbol{\Lambda}_t \tag{2.9}$$

Here $\mathbf{u}$ designates the vector of nodal displacements, $\boldsymbol{\Lambda}_n$ ($\boldsymbol{\Lambda}_t$) the vector of normal (tangential) nodal contact forces, $\mathbf{G}_n$ ($\mathbf{G}_t$) the vector of normal (tangential) nodal gaps, and ω_n (ω_t) the normal (tangential) penalty parameters. Moreover, $\Pi(\mathbf{u})$ stands for the total potential energy of the bodies in contact.

The discrete variational equations are then obtained by taking the variations with respect to $\mathbf{u}$, $\boldsymbol{\Lambda}_n$, and $\boldsymbol{\Lambda}_t$, respectively:

$$\delta_{\mathbf{u}}\Pi(\mathbf{u}) + \boldsymbol{\Lambda}_n^T\delta_{\mathbf{u}}\mathbf{G}_n + \boldsymbol{\Lambda}_t^T\delta_{\mathbf{u}}\mathbf{G}_t = 0 \tag{2.10a}$$

$$\delta\boldsymbol{\Lambda}_n^T\left(-\frac{1}{\omega_n}\boldsymbol{\Lambda}_n + \mathbf{G}_n\right) = 0 \tag{2.10b}$$

$$\delta\boldsymbol{\Lambda}_t^T\left(-\frac{1}{\omega_t}\boldsymbol{\Lambda}_t + \mathbf{G}_t\right) = 0 \tag{2.10c}$$

From (2.10b,c), we obtain that $\boldsymbol{\Lambda}_n = \omega_n\mathbf{G}_n$ and $\boldsymbol{\Lambda}_t = \omega_t\mathbf{G}_t$ as the normal and tangential *penalty* contact forces.

The variation of a typical nodal normal gap $g_n \in \mathbf{G}_n$ takes the form (see Wriggers & Simo [1985])

$$\delta g_n \equiv \boldsymbol{\eta}^T\mathbf{c}_n = [\boldsymbol{\eta}_s - (1-a)\,\boldsymbol{\eta}_1 - a\,\boldsymbol{\eta}_2]\bullet\mathbf{n} \equiv \overline{\boldsymbol{\eta}}\bullet\mathbf{n} \tag{2.11}$$

where $\mathbf{c}_n \equiv \mathbb{D}_{\boldsymbol{\eta}}(\delta g_n)$ ($\mathbb{D}$ is the directional derivative operator). Alternatively, we can write

$$\mathbf{c}_n = \overline{\mathbf{n}}\quad , \tag{2.12}$$

with the "bar" quantity defined in (2.8a). We shall give the matrix representation, within the context of three-node contact elements, of $\overline{\mathbf{n}}$ later in this section.

Similarly, the variation of a typical nodal tangential gap $g_t \in \mathbf{G}_t$ can be obtained according to

$$\delta g_t = (\boldsymbol{\eta}_s - \boldsymbol{\eta}_1)\bullet\mathbf{t} + (\mathbf{x}_s - \mathbf{x}_1)\bullet\delta\mathbf{t} - a''\,\delta\,|\,\mathbf{x}_2 - \mathbf{x}_1\,|$$

$$= \mathbf{t} \bullet \bar{\boldsymbol{\eta}}^{o} + \frac{g_n}{|\mathbf{x}_2 - \mathbf{x}_1|} (\mathbf{n} \bullet \bar{\bar{\boldsymbol{\eta}}}) \equiv \boldsymbol{\eta}^T \mathbf{c}_t \tag{2.13}$$

where

$$\bar{\boldsymbol{\eta}}^{o} \equiv \bar{\boldsymbol{\eta}}\Big|_{a=a^o} = \boldsymbol{\eta}_3 - (1 - a^o)\,\boldsymbol{\eta}_1 - a^o\,\boldsymbol{\eta}_2 \quad , \tag{2.14}$$

and

$$\mathbf{c}_t \equiv \mathbb{D}_{\boldsymbol{\eta}}(\delta g_t) = \bar{\mathbf{t}}^{o} + \frac{g_n}{|\mathbf{x}_2 - \mathbf{x}_1|} \bar{\bar{\mathbf{n}}} \tag{2.15}$$

Moreover, the residual vector $\mathbf{R}_B$ and tangent stiffness $\mathbf{K}_B$ associated with the total potential energy of the contacting bodies simply read

$$\mathbf{R}_B \equiv \mathbb{D}_{\boldsymbol{\eta}}(\Pi(\mathbf{u})) \tag{2.16}$$

$$\mathbf{K}_B \equiv \mathbb{D}_{\boldsymbol{\eta}}(\mathbf{R}_B) \tag{2.17}$$

In the case of *inelasticity*, $\mathbf{R}_B$ and $\mathbf{K}_B$ are deduced from a (Galerkin) variational functional Π involving constitutive relations and boundary conditions.

The variational equations (2.10a,b,c) can now be stated as

$$\boldsymbol{\eta} \left[\mathbf{R}_B + \mathop{\mathbb{A}}_{s=1}^{S} (\lambda_n^{(s)} \mathbf{c}_n^{(s)} + \lambda_t^{(s)} \mathbf{c}_t^{(s)}) \right] = 0 \tag{2.18a}$$

$$\delta \boldsymbol{\Lambda}_n^T (-\frac{1}{\omega_n} \boldsymbol{\Lambda}_n + \mathbf{G}_n) = 0 \tag{2.18b}$$

$$\delta \boldsymbol{\Lambda}_t^T (-\frac{1}{\omega_t} \boldsymbol{\Lambda}_t + \mathbf{G}_t) = 0 \tag{2.18c}$$

In (2.18a), (scalars) $\lambda_n^{(s)} \in \boldsymbol{\Lambda}_n$, $\lambda_t^{(s)} \in \boldsymbol{\Lambda}_t$, and $\mathbb{A}$ represents an assembly operation over all three-node contact elements in consideration (S = total number of slave nodes in contact = total number of conditions of constraints). To apply the Newton's iteration scheme, consistent linearization of Eq. (2.18a,b,c) at ($\mathbf{u}$, $\boldsymbol{\Lambda}_n$, $\boldsymbol{\Lambda}_t$) is performed and leads to

$$[\boldsymbol{\eta}^T , \delta\boldsymbol{\Lambda}_n^T , \delta\boldsymbol{\Lambda}_t^T] \begin{bmatrix} \mathbf{K}_B + \mathop{\mathbb{A}}_{s=1}^{S} [\mathbf{K}_n^{(s)} + \mathbf{K}_t^{(s)}] & \mathop{\mathbb{A}}_{s=1}^{S} \mathbf{c}_n^{(s)} & \mathop{\mathbb{A}}_{s=1}^{S} \mathbf{c}_t^{(s)} \\ \mathop{\mathbb{A}}_{s=1}^{S} \mathbf{c}_n^{(s)T} & -\frac{1}{\omega_n} \mathbf{I} & \mathbf{0} \\ \mathop{\mathbb{A}}_{s=1}^{S} \mathbf{c}_t^{(s)T} & \mathbf{0} & -\frac{1}{\omega_t} \mathbf{I} \end{bmatrix} \begin{Bmatrix} \Delta\mathbf{u} \\ \Delta\boldsymbol{\Lambda}_n \\ \Delta\boldsymbol{\Lambda}_t \end{Bmatrix}$$

$$= - \begin{Bmatrix} \mathbf{R}_B + \mathop{\mathbb{A}}_{s=1}^{S} [\lambda_n^{(s)} \mathbf{c}_n^{(s)} + \lambda_t^{(s)} \mathbf{c}_t^{(s)}] \\ -\frac{1}{\omega_n} \boldsymbol{\Lambda}_n + \mathbf{G}_n \\ -\frac{1}{\omega_t} \boldsymbol{\Lambda}_t + \mathbf{G}_t \end{Bmatrix} \tag{2.19}$$

where (after some algebra)

$$\boldsymbol{\eta}^T \mathbf{K}_n^{(s)} \Delta\mathbf{u} = \frac{-\lambda_n^{(s)}}{|\mathbf{x}_2 - \mathbf{x}_1|} [\, \Delta\bar{\mathbf{u}} \bullet (\mathbf{t} \otimes \mathbf{n}) \bullet \bar{\bar{\boldsymbol{\eta}}} + \bar{\boldsymbol{\eta}} \bullet (\mathbf{t} \otimes \mathbf{n}) \bullet \Delta\bar{\bar{\mathbf{u}}} + \frac{g_n}{|\mathbf{x}_2 - \mathbf{x}_1|} \Delta\bar{\bar{\mathbf{u}}} \bullet (\mathbf{n} \otimes \mathbf{n}) \bullet \bar{\bar{\boldsymbol{\eta}}} \,]^{(s)} \tag{2.20}$$

$$\boldsymbol{\eta}^T \mathbf{K}_t^{(s)} \Delta\mathbf{u} = \frac{\lambda_t^{(s)}}{|\mathbf{x}_2 - \mathbf{x}_1|} [\, \bar{\boldsymbol{\eta}}^o \bullet (\mathbf{n} \otimes \mathbf{n}) \bullet \Delta\bar{\bar{\mathbf{u}}} + \bar{\bar{\boldsymbol{\eta}}} \bullet (\mathbf{n} \otimes \mathbf{n}) \bullet \Delta\bar{\mathbf{u}} - \frac{g_n}{|\mathbf{x}_2 - \mathbf{x}_1|} \bar{\bar{\boldsymbol{\eta}}} \bullet (\mathbf{n} \otimes \mathbf{t} + \mathbf{t} \otimes \mathbf{n}) \bullet \Delta\bar{\bar{\mathbf{u}}} \,]^{(s)} \tag{2.21}$$

2.2.1. Matrix representation. To facilitate finite element implementation of the above derived tangent stiffness operators and residuals, matrix formulations are given as follows. For simplicity, we will drop the superscript (s) and focus on a typical single three-node element. Let us start by introducing the following vectors

$$\mathbf{N}_s^o \equiv [\mathbf{n} , -(1 - a^o)\,\mathbf{n} , -a^o\,\mathbf{n}]^T \tag{2.22a}$$

$$\mathbf{N}_s \equiv \mathbf{c}_n \equiv \bar{\mathbf{n}} \equiv [\mathbf{n} , -(1 - a)\,\mathbf{n} , -a\,\mathbf{n}]^T \tag{2.22b}$$

$$\mathbf{T}_s \equiv [\mathbf{t} , -(1 - a)\,\mathbf{t} , -a\,\mathbf{t}]^T \tag{2.22c}$$

$$\mathbf{T} \equiv \bar{\bar{\mathbf{t}}} \equiv [\mathbf{0} , -\mathbf{t} , \mathbf{t}]^T \tag{2.22d}$$

$$\mathbf{N} \equiv \bar{\bar{\mathbf{n}}} \equiv [\mathbf{0} , -\mathbf{n} , \mathbf{n}]^T \tag{2.22e}$$

$$\Delta\mathbf{u} \equiv [\Delta\mathbf{u}_s , \Delta\mathbf{u}_1 , \Delta\mathbf{u}_2]^T \tag{2.22f}$$

$$\mathbf{c}_t \equiv [\mathbf{t} , -(1 - a^o)\,\mathbf{t} - \frac{g_n}{|\mathbf{x}_2 - \mathbf{x}_1|}\,\mathbf{n} , -a^o\,\mathbf{t} + \frac{g_n}{|\mathbf{x}_2 - \mathbf{x}_1|}\,\mathbf{n}]^T \tag{2.22g}$$

where the unified order of components in all vectors has been: slave node - master node 1 - master node 2. By using these matrix notations, Eq. (2.20) and (2.21) can be rephrased as

$$\mathbf{K}_n = -\frac{\lambda_n}{|\mathbf{x}_2 - \mathbf{x}_1|} [\mathbf{N}\,\mathbf{T}_s^T + \mathbf{T}_s\,\mathbf{N}^T + \frac{g_n}{|\mathbf{x}_2 - \mathbf{x}_1|}\,\mathbf{N}\,\mathbf{N}^T] \tag{2.23}$$

$$\mathbf{K}_t = \frac{\lambda_t}{|\mathbf{x}_2 - \mathbf{x}_1|} [\mathbf{N}_s^o\,\mathbf{N}^T + \mathbf{N}\,\mathbf{N}_s^T - \frac{g_n}{|\mathbf{x}_2 - \mathbf{x}_1|}(\mathbf{N}\,\mathbf{T}^T + \mathbf{T}\,\mathbf{N}^T)] \tag{2.24}$$

In addition, from Eq. (2.19) together with the fact that $\lambda_n = \omega_n\, g_n$ and $\lambda_t = \omega_t\, g_t$, the contact residual vector (due to contact only) for a single element is

$$\mathbf{R}_C = -[\omega_n\, g_n\, \mathbf{c}_n + \omega_t\, g_t\, \mathbf{c}_t] \tag{2.25}$$

The linearization of Eq. (2.25) with respect to $\mathbf{u}$ in conjunction with Eq. (2.19) then leads to the following *perturbed Lagrangian* contact tangent stiffness matrix

$$\mathbf{K}_t = \omega \left\{ [\mathbf{N}_s\,\mathbf{N}_s^T + \mathbf{c}_t\,\mathbf{c}_t^T] - \frac{g_n}{|\mathbf{x}_2 - \mathbf{x}_1|} [\mathbf{N}\,\mathbf{T}_s^T + \mathbf{T}_s\,\mathbf{N}^T + \frac{g_n}{|\mathbf{x}_2 - \mathbf{x}_1|}\,\mathbf{N}\,\mathbf{N}^T] \right.$$

$$\left. - \frac{\varepsilon}{|\mathbf{x}_1 - \mathbf{x}_2|} (\mathbf{N}\,\mathbf{N}^T + \mathbf{N}\,\mathbf{N}^T - \frac{g_n}{|\mathbf{x}_1 - \mathbf{x}_2|} (\mathbf{N}\,\mathbf{T}^T + \mathbf{T}\,\mathbf{N}^T)) \right\} \tag{2.26}$$

Here, $\varepsilon_n = \varepsilon_t = \varepsilon$ (penalty parameter) has been assumed. Finally, the *total* tangent stiffness matrix and residual vector of the bodies in contact take the form

$$\mathbf{K} = \mathbf{K}_B + \mathop{A}_{s=1}^{S} \mathbf{K}_C^{(s)} \tag{2.27}$$

$$\mathbf{R} = - [\, \mathbf{R}_B + \mathop{A}_{s=1}^{S} \omega\, (g_n\, \mathbf{c}_n + g_t\, \mathbf{c}_t)^{(s)} \,] \tag{2.28}$$

Remark 2.1. From Eq. (2.23), we observe that $\mathbf{K}_n$ is *symmetric*. By contrast, from (2.24), $\mathbf{K}_t$ (and hence $\mathbf{K}_C$ in (2.26)) is *non-symmetric* as long as $\mathbf{N}_s^o \neq \mathbf{N}_s$. That is, only when $\alpha = \alpha$ will $\mathbf{K}_t$ be symmetric. This situation arises only when the final numerical convergence is achieved for the frictional non-slip case. □

Remark 2.2. If one drops the nonlinear terms ($\mathbf{K}_n$, $\mathbf{K}_t$) from (2.26), then the *linearized* theory is recovered. In other words, only the rank-one-update term $w\,[\mathbf{N}_s\,\mathbf{N}_s^T + \mathbf{c}_t\,\mathbf{c}_t^T]$ remains. □

2.3. Frictional slip

For the case of frictional slide, use of the Coulomb's law of friction renders $\mathbf{\Lambda}_t = \mu\, \mathbf{\Lambda}_n$, where μ denotes the coefficient of friction. Similar to the development in Sec. 2.2, characteristic variational equations are:

$$\delta_{\mathbf{u}}\Pi(\mathbf{u}) + \mathbf{\Lambda}_n^T \delta_{\mathbf{u}}\mathbf{G}_n - \mu\, \mathbf{\Lambda}_n^T \delta_{\mathbf{u}}\mathbf{G}_t = 0 \tag{2.29a}$$

$$\delta\mathbf{\Lambda}_n^T (-\frac{1}{\omega}\mathbf{\Lambda}_n + \mathbf{G}_n) = 0 \tag{2.29b}$$

in which ω is a penalty parameter. Note that in Eq. (2.29a) the virtual work done by the frictional force is always *negative*. Furthermore, Eq. (2.29b) yields $\mathbf{\Lambda}_n = \omega\, \mathbf{G}_n$ as the normal penalty contact force.

By taking the variations at $(\mathbf{u}\,,\,\mathbf{\Lambda}_n)$, Eq. (2.29a,b) now read (see (2.18a,b,c))

$$\boldsymbol{\eta} \left[\mathbf{R}_B + \mathop{A}_{s=1}^{S} (\Lambda_n^{(s)}\, \mathbf{c}_n^{(s)} - \mu\, \Lambda_n^{(s)}\, \mathbf{c}_t^{(s)}) \right] = 0 \tag{2.30a}$$

$$\delta\mathbf{\Lambda}_n^T (-\frac{1}{\omega}\mathbf{\Lambda}_n + \mathbf{G}_n) = 0 \tag{2.30b}$$

The consistent linearization of (2.30a,b) at $(\mathbf{u}\,,\,\mathbf{\Lambda}_n)$ then yields the following expressions (see (2.19)):

$$[\boldsymbol{\eta}^T \;\; \delta\mathbf{\Lambda}_n^T] \begin{bmatrix} \mathbf{K}_B + \mathop{A}_{s=1}^{S} [\mathbf{K}_{\cdot\cdot} + \mathbf{K}^{\cdot\cdot}] & \mathop{A}_{s=1}^{S} [\mathbf{c}_{\cdot\cdot} - \mu\, \mathbf{c}_{\cdot\cdot}] \\ \mathop{A}_{s=1}^{S} \mathbf{c}_{\cdot\cdot} & -\frac{1}{\omega}\mathbf{I} \end{bmatrix} \begin{Bmatrix} \Delta\mathbf{u} \\ \Delta\mathbf{\Lambda}_n \end{Bmatrix}$$

$$= - \begin{Bmatrix} \mathbf{R}_B + \mathop{A}_{s=1}^{S} [\lambda_n^{(s)} \mathbf{c}_n^{(s)} - \mu \lambda_n^{(s)} \mathbf{c}_t^{(s)}] \\ -\frac{1}{\omega} \boldsymbol{\Delta}_n + \mathbf{G}_n \end{Bmatrix} \tag{2.31}$$

Here, $\mathbf{K}_n$ is the same as Eq. (2.20) and (2.23), whereas $\mathbf{K}_t$ takes the following matrix form (for a single element)

$$\mathbf{K}_t = - \frac{\mu \lambda_n}{|\mathbf{x}_2 - \mathbf{x}_1|} [\mathbf{N}_s^o \mathbf{N}^T + \mathbf{N} \mathbf{N}_s^T - \frac{g_n}{|\mathbf{x}_2 - \mathbf{x}_1|} (\mathbf{N} \mathbf{T}^T + \mathbf{T} \mathbf{N}^T)] \tag{2.32}$$

It is noted that Eq. (2.32) can be obtained by simply replace λ_t in Eq. (2.24) by $[-\mu \lambda_n]$, as a direct consequence of the Coulomb's friction law.

Remark 2.3. If the surface coordinate $a \approx a^o$ (i.e., approximately unchanged), then $\mathbf{N}_s^o \approx \mathbf{N}_s$ and $\mathbf{K}_t$ is almost symmetric. □

Since $\lambda_n = \omega g_n$, the contact residual for one element is

$$\mathbf{R}_C = - \omega g_n [\mathbf{c}_n - \mu \mathbf{c}_t] \tag{2.33}$$

The linearization of (2.33) at $\mathbf{u}$ together with Eq. (2.31),(2.32),(2.23) then yield the contact tangent stiffness for frictional slip:

$$\mathbf{K}_C = \omega \left\{ [\mathbf{N}_s \mathbf{N}_s^T - \mu \mathbf{c}_t \mathbf{N}_s^T] - \frac{g_n}{|\mathbf{x}_2 - \mathbf{x}_1|} [\mathbf{N} \mathbf{T}_s^T + \mathbf{T}_s \mathbf{N}^T + \frac{g_n}{|\mathbf{x}_2 - \mathbf{x}_1|} \mathbf{N} \mathbf{N}^T] \right.$$
$$\left. - \frac{\mu g_n}{|\mathbf{x}_2 - \mathbf{x}_1|} [\mathbf{N}_s^o \mathbf{N}^T + \mathbf{N} \mathbf{N}_s^T - \frac{g_n}{|\mathbf{x}_2 - \mathbf{x}_1|} (\mathbf{N} \mathbf{T}^T + \mathbf{T} \mathbf{N}^T)] \right\} \tag{2.34}$$

Therefore, the *total* tangent stiffness matrix and residual vector associated with the contacting bodies are

$$\mathbf{K} = \mathbf{K}_B + \mathop{A}_{s=1}^{S} \mathbf{K}_C^{(s)} \tag{2.35}$$

$$\mathbf{R} = - [\mathbf{R}_B + \mathop{A}_{s=1}^{S} \omega g_n (\mathbf{c}_n - \mu \mathbf{c}_t)^{(s)}] \tag{2.36}$$

Remark 2.4. It is seen from Eq. (2.34) that the contact tangent stiffness for the case of frictional sliding is always *non-symmetric* due to the nature of the Coulomb's friction law. Even in the event of linearized kinematics (i.e., by neglecting nonlinear terms $\mathbf{K}_n$ and $\mathbf{K}_t$), this is still the case (see also Oden & Martins [1985]). □

3. Numerical implementation and examples

In this section, implementation of the proposed formulation within the context of the finite element method is described. Some numerical examples are also presented.

3.1. Finite element implementation

The "master-slave" slide-line contact logic is employed, which features both the "one-pass" and "two-pass" algorithms (see, e.g., Hallquist [1983]). For the planar three-node contact element under consideration, explicit vector-component expressions (6 d.o.f.) for the notations defined in Eq. (2.22a-g) can be obtained. For example,

$$\mathbf{N}_s \equiv \mathbf{c}_n = \begin{Bmatrix} -s \\ c \\ (1-a)s \\ -(1-a)c \\ a\,s \\ -a\,c \end{Bmatrix} \quad ; \quad \mathbf{c}_t = \begin{Bmatrix} c \\ s \\ -(1-a^o)c + \dfrac{g_n}{|\mathbf{x}_2-\mathbf{x}_1|}s \\ -(1-a^o)s - \dfrac{g_n}{|\mathbf{x}_2-\mathbf{x}_1|}c \\ -a^o c - \dfrac{g_n}{|\mathbf{x}_2-\mathbf{x}_1|}s \\ -a^o s + \dfrac{g_n}{|\mathbf{x}_2-\mathbf{x}_1|}c \end{Bmatrix} \tag{3.1}$$

where s , c denote $\sin\theta$, $\cos\theta$, respectively (see Fig. 1).

In the spirit of operator splitting methodology for the Coulomb's law of friction, each load (time) step is decomposed into two parts : (i) By assuming a sticking condition, a "*stick trial*" step is first performed (similar to the "elastic trial" step in classical elastoplasticity). If the trial is successful, the contacting bodies are considered to be in a state of frictional sticking. Otherwise, (ii) a "*slip correction*" step is performed (similar to the "plastic return mapping" step in elastoplasticity) and the bodies in contact are viewed to be in a state of frictional sliding. This operator split treatment separates the no-slip and slip conditions and renders the transition from stick to slip (or vice versa) exactly the same way as the corresponding case in classical elastoplasticity. The analogy between the Coulomb's law of friction (for stick-slip contact problems) and yield criterion (for elastoplasticity) is noted

In all numerical examples that follow, standard Newton's method is used for solution procedure. It is emphasized that line search plays no role in numerical simulations presented in this section.

3.2. Example 1: frictional stick

This section is concerned with a (rigid or deformable) punch into an elastic foundation under the circumstance of frictional stick. See Figure 2 for (plane strain) finite element mesh and dimensions.

Case 1. Rigid punch. The material properties employed in the computation are: $E_{punch} = 10^8$ (assumed rigid), $\nu_{punch} = 0$, $E_{ground} = 10^5$, $\nu_{ground} = 0.3$, and $\omega = 10^7$ (penalty value). The one-pass algorithm is used in this example. The finite element solutions converge *quadratically* within 4 iterations; see Table 1 for numerical performance. The deformed mesh is displayed in Figure 3, in which the deformation is enlarged 1000 times the real scale in

order to fully see the details.

Table 1. *Residual & energy norms for iterates*

Iteration	1	2	3	4
Residual	.245e+4	.299e+3	.719e-1	.173e-6
Energy	.552e+2	.151e+0	.692e-10	.727e-19

Case 2. Elastic punch. The punching block is now a deformable body. The material properties involved in the computation are: $E_{punch} = 10^4$, $\nu_{punch} = 0.3$, $E_{found} = 10^3$, $\nu_{found} = 0.3$, and $\omega = 10^7$ (penalty value). The one-pass algorithm is adopted in this example. Once again, the finite element solutions converge *quadratically* within 3 iterations; see Table 2 for numerical performance. The deformed mesh is displayed in Figure 4 (to scale).

Table 2. *Residual & energy norms for iterates*

Iteration	1	2	3
Residual	.245e+4	.528e+2	.155e-4
Energy	.682e+4	.217e-4	.116e-12

3.3. Example 2: frictional slide

Attention is now focused on the event of frictional stick-slip motion. The transition from stick to slip (or vice versa) is accounted for in this example. We once more consider an elastic punch on top of an elastic foundation made of same materials. The finite element mesh and boundary conditions are the same as Sec. 3.2 (see Fig. 2). Moreover, the material properties used in the simulation are: $E = 10^4$, $\nu = 0$, and $\omega = 10^5$, $\mu = 0.1$ (coefficient of friction).

The punch is first vertically loaded into the elastic foundation, then move horizontally to the right by displacement controlled loading condition (vertical loads still remain). During the initial vertical loading, three bottom nodes of the punch are in contact with the foundation. In particular, the two (outer) edge nodes of the punch undergo frictional *slip* while the central node experiences frictional *stick*. The solutions converge in 7 iterations with a residual norm less than 10^{-3}. Within the proposed formulation and implementation, tangential motion across element boundaries does not impose numerical difficulties.

Before the first contact node (the rightmost contact node) of the punch reaches the right edge of the foundation, a typical iteration count for numerical convergence is 6 or 7. After the first punch element begins to overhang, the contact area is not constant and the number of contacting nodes changes. At 5% overhang (of the first punch element), the convergence takes 7 iterations. See Fig. 5 for deformed configuration (to scale). At 50% overhang, 8 iterations are taken before convergence is achieved. At 80% overhang, 11 iterations are recorded. At 90% overhang, 13 iterations are required. Finally, at 98% and 100% overhang, 15 iterations are observed. See Figures 6, 7 for deformed meshes (to scale). After the first punch element completely overhangs, the solutions diverge which corresponds to the physical drop-off process of the punch. For this simulation, it is *crucial* to use the *two-pass* algorithm for a solution to converge. The one-pass algorithm works only before the punch overhangs. This example provides a severe test for finite element formulation of frictional contact problems.

To assess the significance of the proposed *consistent* tangent stiffness, we repeat the above numerical experiment by using the *linearized* tangent (i.e., employing only the rank-one-update terms). Before the first punch element overhangs, numerical convergence typically takes 8 or 9 iterations. At 5% overhang, the convergence takes 9 iterations. At 50% overhang, 11 iterations are observed before convergence is achieved. At 80% overhang, 19 iterations are recorded. At 90% overhang, 25 iterations are required. Finally, at 100% overhang, 33 iterations are observed. The significance of the proposed formulation versus linearized theory is clearly demonstrated.

4. Conclusion

On the basis of an operator split, the proposed formulation accommodates the frictional stick-slip motion in a variational framework. By a consistent linearization procedure, explicit expressions for the consistent contact tangent stiffness and residual have been obtained. The analogy between the proposed treatment for the stick-slip motion and the corresponding treatment in classical elasto-plasticity is noteworthy. In addition, for infinitesimal deformations (as a special case), the proposed formulation reduces to the linearized theory involving only rank-one-update terms in the tangent matrices.

To illustrate the numerical performance of the proposed formulation, some numerical examples have been presented in Sec. 3. The significant role of the proposed tangent stiffness is fully demonstrated.

Acknowledgments. This work is sponsored by Naval Civil Engineering Laboratory with the University of California, Berkeley. This support and the continued interest of Dr. Ted Shugar is gratefully acknowledged.

References

Duvaut, G. and Lions, J.L. [1976], *Inequalities in Mechanics and Physics,* Springer, Berlin.

Hallquist, J.O. [1983], "NIKE2D - A vectorized, implicit, finite deformation, finite element code for analyzing the static and dynamic response of 2-D solids," Rept. UCID-19677, Lawrence Livermore National Laboratory.

Hughes, T.R.J., Taylor, R.L., Sackman, J.L., Curnier, A. and Kanoknukulchai, W., [1976], "A finite element method for a class of contact-impact problems," *Comp. Meth. Appl. Mech. Engng.,* **8**, pp. 249-276.

Landers, J.A. and Taylor, R.L. [1985], "An augmented Lagrangian formulation for the finite element solution of contact problems," Rept. No. UCB/SESM-85/09, Dept. of Civil Engng., University of California, Berkeley.

Michalowski, R. and Mroz, Z. [1978], "Associated and non-associated sliding rules in contact friction problems," *Arch. of Mech.,* **30**, pp. 259-276.

Oden, J.T. and Lin, T.L. [1986], "On the general rolling contact problem for finite deformations of a viscoelastic cylinder," *Comp. Meth. Appl. Mech. Engng.,* **57**, pp. 297-367.

Oden, J.T. and Martins, J.A.C. [1985], "Models and computational methods for dynamic friction phenomena," *Comp. Meth. Appl. Mech. Engng.,* **52**, pp. 527-634.

Oden, J.T. and Pires, E.B. [1984], "Nonlocal friction in contact problems in plane elasticity," in *Finite Elements,* Vol. 5, *Special Problems in Solid Mechanics,* Prentice-Hall, Inc..

Simo, J.C., Wriggers, P., and Taylor, R.L. [1985], "A perturbed Lagrangian formulation for the finite element solution of contact problems," *Comp. Meth. Appl. Mech. Engng.,* **50**, pp. 163-180.

Tabor, D., [1981], "Friction - the present state of our understanding," *J. Lubrication Technology,* **103**, pp. 169-179.

Wriggers, P. and Simo, J.C. [1985], "A note on tangent stiffness for fully nonlinear contact problems," *Commun. Appl. Numer. Meth.,* **1**, pp. 199-203.

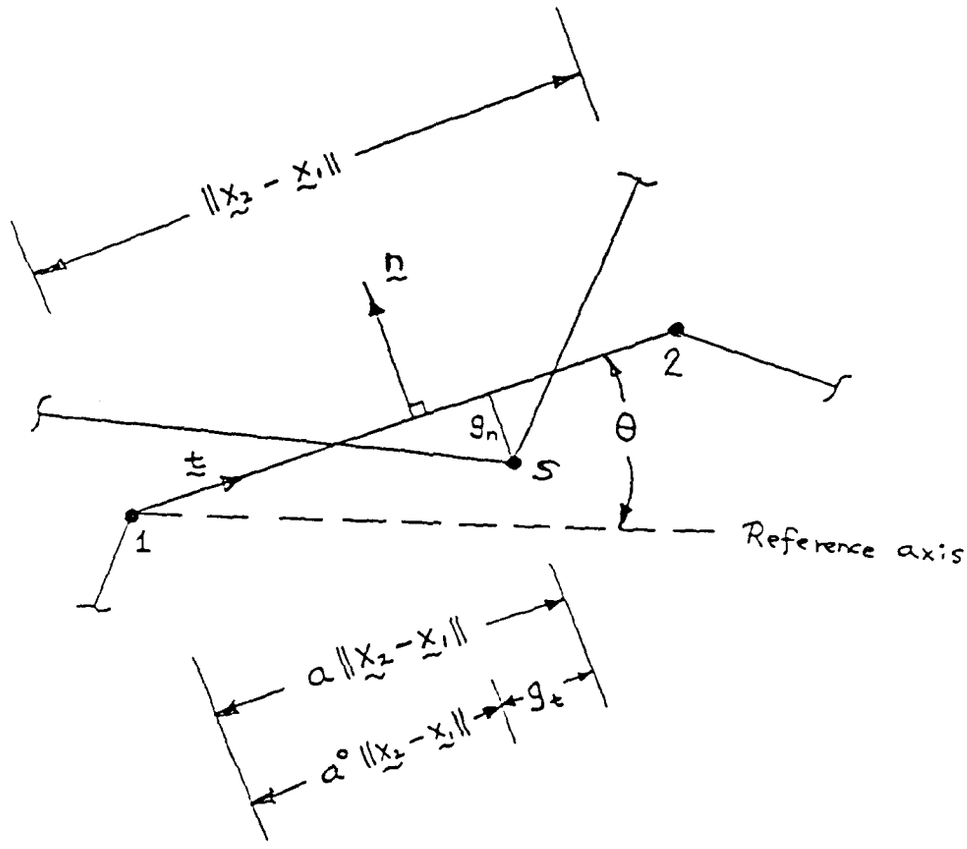

Figure 1. Geometry and definition of a typical three-node contact element.

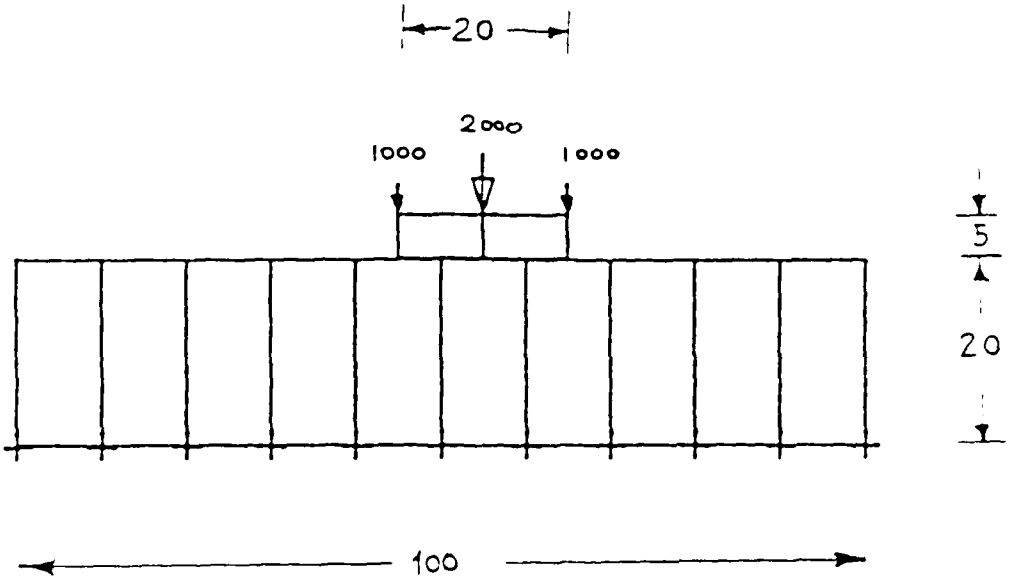

Figure 2. Finite element mesh (including boundary conditions and loads) for a punch on top of a foundation.

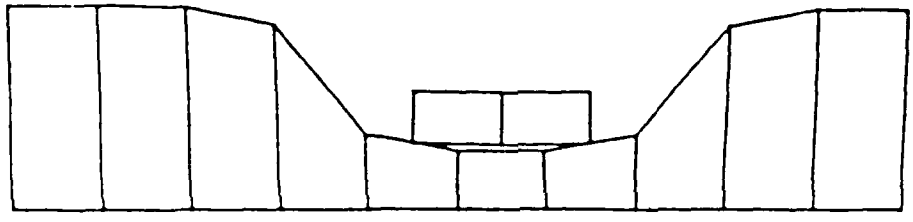

Figure 3. Deformed mesh for a rigid punch into an elastic foundation. The deformation is enlarged 1000 times for clarity.

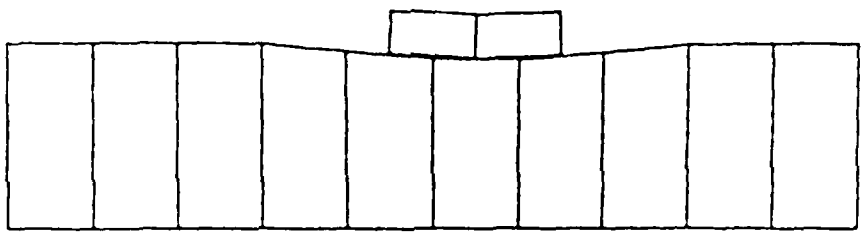

Figure 4. Deformed mesh for an elastic punch into an elastic foundation.

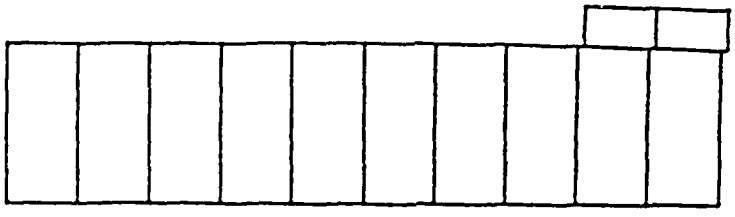

Figure 5. Deformed mesh corresponding to 5% overhang of the first (right) element of the punch.

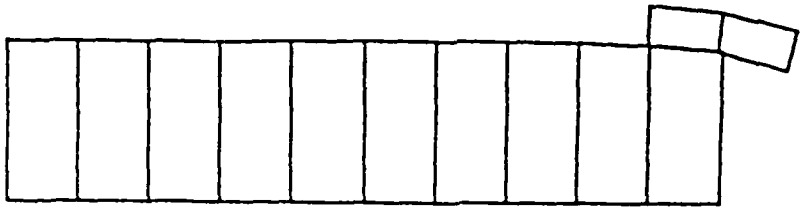

Figure 6. Deformed mesh corresponding to 98% overhang of the first punch element.

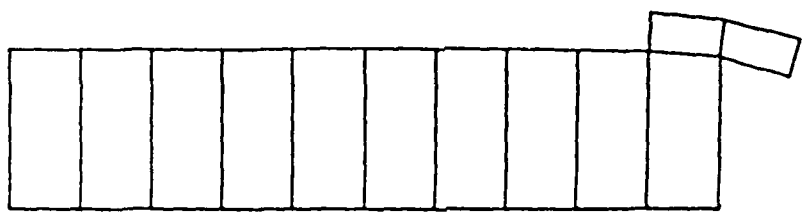

Figure 7. Deformed mesh corresponding to 100% overhang of the first punch element.

DISTRIBUTION LIST

DTIC Alexandria, VA
GIDEP OIC, Corona, CA
NAVFACENGCOM Code 03, Alexandria, VA
NAVFACENGCOM - CHES DIV, Code FPO-1PL, Washington, DC
NAVFACENGCOM - LANT DIV, Library, Norfolk, VA
NAVFACENGCOM - NORTH DIV, Code 04AL, Philadelphia, PA
NAVFACENGCOM - PAC DIV, Library, Pearl Harbor, HI
NAVFACENGCOM - SOUTH DIV, Library, Charleston, SC
NAVFACENGCOM - WEST DIV, Library (Code 04A2.2), San Bruno, CA
PWC Code 101 (Library), Oakland, CA; Code 123-C, San Diego, CA; Code 420, Great Lakes, IL; Library (Code 134), Pearl Harbor, HI; Library, Guam, Mariana Islands; Library, Norfolk, VA; Library, Pensacola, FL; Library, Yokosuka JA; Tech Library, Subic Bay, RP

END

5-87

DTIC